

## SUPPLEMENTARY INFORMATION

### **The *P. aeruginosa* effector Tse5 forms membrane pores disrupting the membrane potential of intoxicated bacteria**

**Amaia González-Magaña<sup>1,#</sup>, Jon Altuna<sup>1,#</sup>, María Queralt-Martín<sup>2</sup>, Eneko Largo<sup>1,3</sup>, Carmen Velázquez<sup>1</sup>, Itxaso Montánchez<sup>3</sup>, Patricia Bernal<sup>4</sup>, Antonio Alcaraz<sup>2</sup>, David Albesa-Jové<sup>1,5\*</sup>**

<sup>1</sup> Instituto Biofisika (CSIC, UPV/EHU), Fundación Biofísica Bizkaia/Biofisika Bizkaia Fundazioa (FBB) and Departamento de Bioquímica y Biología Molecular, University of the Basque Country, 48940 Leioa, Spain.

<sup>2</sup> Laboratory of Molecular Biophysics, Department of Physics, University Jaume I, 12071 Castellón, Spain

<sup>3</sup> Departamento de Inmunología, Microbiología y Parasitología, University of the Basque Country, 48940 Leioa, Spain.

<sup>4</sup> Departamento de Microbiología, Facultad de Biología, Universidad de Sevilla, 41012 Sevilla, Spain

<sup>5</sup> Ikerbasque, Basque Foundation for Science, 48013 Bilbao, Spain

# These authors contributed equally to this work

Running title: Tse5 forms ion-selective pores to depolarise intoxicated bacterial cells

\* To whom correspondence should be addressed: David Albesa-Jové, Instituto Biofisika (UPV/EHU, CSIC), Scientific Park of the University of the Basque Country, Leioa, E-48940, Spain; Phone: +34 94 601 5171; E-mail: [david.albesa@ehu.eus](mailto:david.albesa@ehu.eus)

## TABLE OF CONTENTS

|   |    |
|---|----|
| <i>Supplementary Results</i> .....  | 3  |
| <i>Tse5 contributes to the antibacterial activity of P. aeruginosa when competing against P. putida</i> ..... | 3  |
| <i>Supplementary Tables</i> .....   | 4  |
| <i>Supplementary Table 1. Conductances obtained from I-V curves</i> .....                                     | 4  |
| <i>Supplementary Table 2. Strains and Plasmids used in this study</i> .....                                   | 4  |
| <i>Supplementary Figures</i> .....  | 7  |
| <i>Supplementary Note 1 LC-ESI-MS report for Tse5-CT</i> .....  | 14 |
| <i>Supplementary Note 2 N-terminal sequencing report</i> .....  | 18 |
| <i>Supplementary references</i> .....   | 26 |

## Supplementary Results

### **Tse5 contributes to the antibacterial activity of *P. aeruginosa* when competing against *P. putida***

*In vitro* competition assays were performed on LB Lennox (5 g/L NaCl) agar (1.5% w/v) plates, as previously described<sup>1</sup>. Briefly, overnight bacterial cultures were washed and adjusted to an OD<sub>600</sub> of 10 in sterile PBS and mixed in a 1:1 ratio (*P. aeruginosa* (attacker) : *P. putida* (prey)). To differentiate the antibacterial activity of Tse5 from other T6SS effectors, we employed three *P. aeruginosa* knockouts: *P. aeruginosa*  $\Delta retS$ ,  $\Delta retS \Delta vgrG1$ , and  $\Delta retS \Delta tse5$ . The *P. aeruginosa* : *P. putida* mixtures were grown on LB agar plates at 30 °C for 5 hours and then collected using an inoculating loop and resuspended in sterile PBS. The outcome of the competition was quantified by counting colony forming units (CFUs) using antibiotic selection at 5 hours. The prey strain *P. putida* KT2440R harbours a mini-Tn7 transposon<sup>2</sup> inserted at the *attTn7* site on the chromosome that confers resistance to gentamicin and was used for antibiotic selection. Seventeen biologically independent experiments were performed.

The bacterial competition assays show the antibacterial activity of *P. aeruginosa* effectors secreted by the T6SS (Supplementary Fig. 1). *P. putida* survival increases by 0.45 logs when VgrG1-dependent effectors are not secreted ( $\Delta retS \Delta vgrG1$ ), while survival increases 0.25 logs when Tse5 is not present ( $\Delta retS \Delta tse5$ ). Although these survival increments are small, they are statistically significant, providing experimental evidences of the Tse5 antibacterial activity during bacterial competition.

## Supplementary Tables

**Supplementary Table 1. Conductances obtained from I-V curves**

| <i>E. coli</i><br>250/50<br>mM | <i>E. coli</i><br>50/250<br>mM | Neutral<br>250/50<br>mM |
|--------------------------------|--------------------------------|-------------------------|
| 0.57 nS                        | 0.99 nS                        | 0.95 nS                 |
| 0.57 nS                        | 1.10 nS                        | 6.62 nS                 |
| 1.54 nS                        | 2.22 nS                        |                         |
| 1.76 nS                        | 4.49 nS                        |                         |
| 1.78 nS                        |                                |                         |
| 1.83 nS                        |                                |                         |

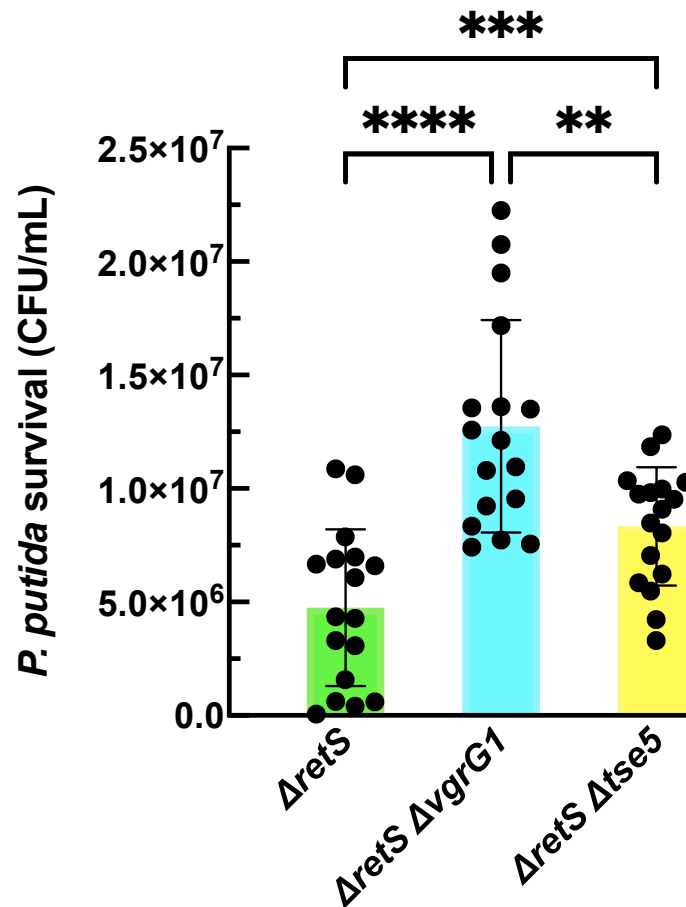
**Supplementary Table 2. Strains and Plasmids used in this study**

| Strain   | Relevant characteristics   | Use   | Origin       |
|--|--|---|--------------|
| <b><i>E. coli</i></b>  |  |   |              |
| <b>DH5<math>\alpha</math></b>                                | <i>F</i> - <i>endA1 glnV44 thi-1 recA1 relA1 gyrA96 deoR nupG purB20 <math>\phi</math>80dlacZ <math>\Delta</math>M15 <math>\Delta</math>(lacZYA- argF)U169, hsdR17 (r K-mK+), <math>\lambda</math>-</i>                                  | <i>In vivo</i> study of Tse5-CT TM regions using PhoA-LacZ $\alpha$ dual reporter | Invitrogen   |
| <b>Lemo21</b>  | BL21(DE3) strain with an extra plasmid harbouring the gene encoding T7 lysozyme, an inhibitor of the T7 RNAP, under control of the well-titratable rhamnose promoter   | Heterologous expression of Tse5 for purification of Tse5-CT                       | <sup>3</sup> |
| <b><i>P. putida</i></b>                                      |  |   |              |
| <b>EM383</b>   | mt-2 derivative cured of the TOL plasmid pWW0 $\Delta$ prophage1 $\Delta$ prophage4 $\Delta$ prophage3 $\Delta$ prophage2 $\Delta$ Tn7 $\Delta$ endA-1 $\Delta$ endA-2 $\Delta$ hsdRMS $\Delta$ flagellum, $\Delta$ Tn4652 $\Delta$ recA | Flow cytometry and growth inhibition studies                                      | <sup>4</sup> |
| <b>KT2440R</b>   | Harbours a mini-Tn7 transposon inserted at the <i>attTn7</i> site on the chromosome that confers resistance to gentamicin  | It was used for antibiotic selection in the bacterial competition assay           | This work    |
| <b><i>P. aeruginosa</i></b>                                  |  |   |              |
| <b>PAO1 <math>\Delta</math>retS</b>                          | Knockout mutant with activated H1-T6SS   | It was used as attacker in the bacterial competition assay                        | <sup>5</sup> |
| <b>PAO1 <math>\Delta</math>retS <math>\Delta</math>vgrG1</b> | Knockout mutant with activated H1-T6SS and deleted <i>vgrG1</i> gene   | It was used as attacker in the bacterial competition assay                        | <sup>5</sup> |

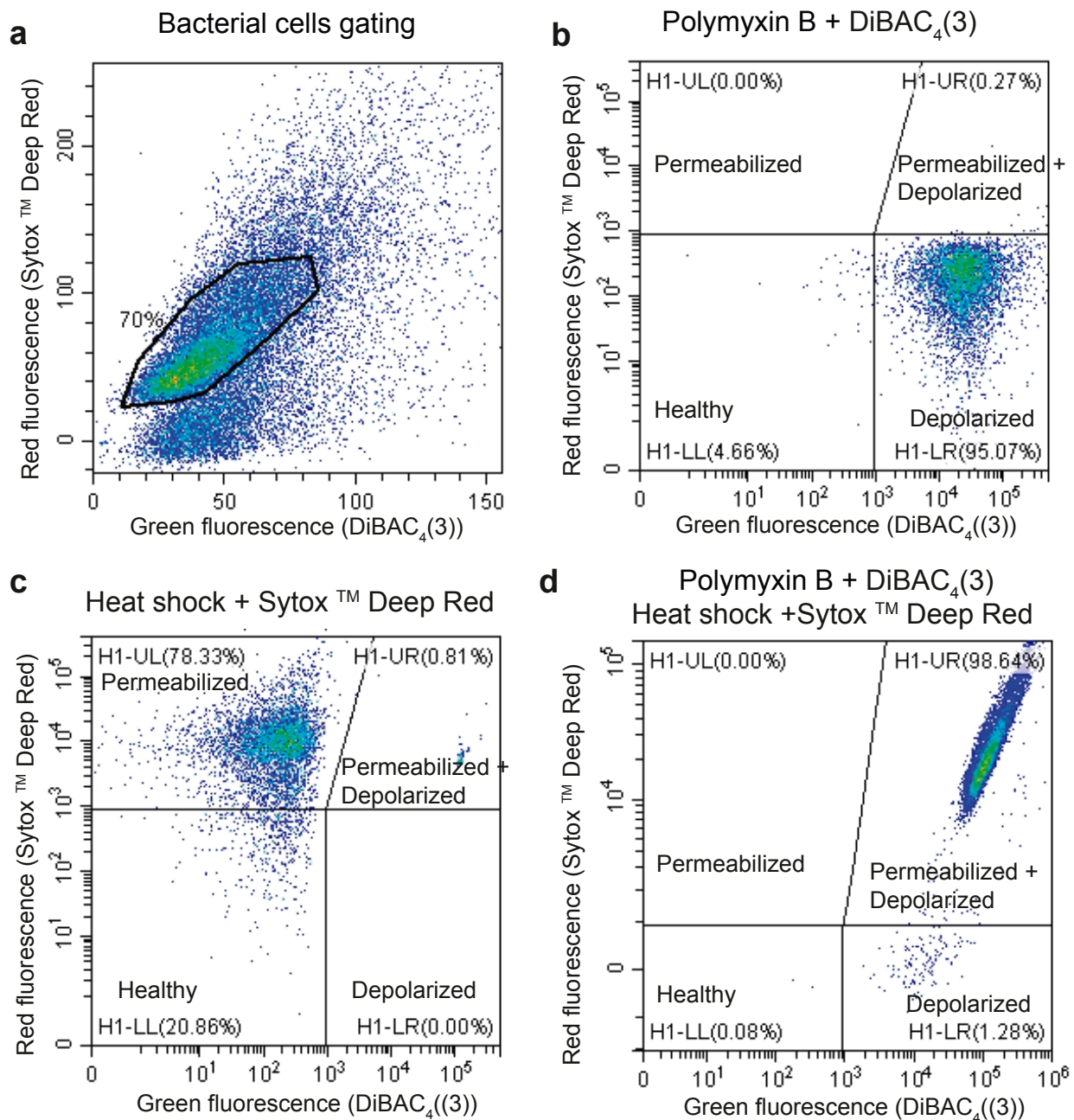
| PAO1 $\Delta retS \Delta tse5$                | Knockout mutant with activated H1-T6SS and deleted <i>tse5</i> gene   | It was used as attacker in the bacterial competition assay | 5               |
|---|---|--|-----------------|
| Plasmid                                       | Relevant characteristics  | Use  | Origin          |
| pKTop   | A vector expressing the reporter protein PhoA <sub>22-472</sub> / LacZ <sub>4-50</sub> , p15 ori; Km <sup>r</sup>   | Parental vector  | 6               |
| pKTop:: <i>sptse5-CT</i> <sub>1169-1229</sub> | Derived from pKTop expressing the Tse5-CT <sub>1169-1229</sub> / PhoA <sub>22-472</sub> / LacZ <sub>4-60</sub> fusion protein <b>with the PelB</b> signal peptide fused at the N-terminus | Membrane insertion   | This work study |
| pKTop:: <i>sptse5-CT</i> <sub>1169-1269</sub> | Derived from pKTop expressing the Tse5-CT <sub>1169-1269</sub> / PhoA <sub>22-472</sub> / LacZ <sub>4-60</sub> fusion protein <b>with the PelB</b> signal peptide fused at the N-terminus | Membrane insertion   | This work study |
| pKTop:: <i>sptse5-CT</i> <sub>1169-1281</sub> | Derived from pKTop expressing the Tse5-CT <sub>1169-1281</sub> / PhoA <sub>22-472</sub> / LacZ <sub>4-60</sub> fusion protein <b>with the PelB</b> signal peptide fused at the N-terminus | Membrane insertion   | This work study |
| pKTop:: <i>sptse5-CT</i> <sub>1169-1300</sub> | Derived from pKTop expressing the Tse5-CT <sub>1169-1300</sub> / PhoA <sub>22-472</sub> / LacZ <sub>4-60</sub> fusion protein <b>with the PelB</b> signal peptide fused at the N-terminus | Membrane insertion   | This work study |
| pKTop:: <i>sptse5-CT</i> <sub>1169-1317</sub> | Derived from pKTop expressing the Tse5-CT <sub>1169-1317</sub> / PhoA <sub>22-472</sub> / LacZ <sub>4-60</sub> fusion protein <b>with the PelB</b> signal peptide fused at the N-terminus | Membrane insertion   | This work study |
| pKTop:: <i>tse5-CT</i> <sub>1169-1229</sub>   | Derived from pKTop expressing the Tse5-CT <sub>1169-1229</sub> / PhoA <sub>22-472</sub> / LacZ <sub>4-60</sub> fusion protein <b>without PelB</b> signal peptide                          | Membrane insertion   | This work study |
| pKTop:: <i>tse5-CT</i> <sub>1169-1269</sub>   | Derived from pKTop expressing the Tse5-CT <sub>1169-1269</sub> / PhoA <sub>22-472</sub> / LacZ <sub>4-60</sub> fusion protein <b>without the PelB</b> signal peptide                      | Membrane insertion   | This work study |
| pKTop:: <i>tse5-CT</i> <sub>1169-1281</sub>   | Derived from pKTop expressing the Tse5-CT <sub>1169-1281</sub> / PhoA <sub>22-472</sub> / LacZ <sub>4-60</sub> fusion protein <b>without the PelB</b> signal peptide                      | Membrane insertion   | This work study |
| pKTop:: <i>tse5-CT</i> <sub>1169-1300</sub>   | Derived from pKTop expressing the Tse5-CT <sub>1169-1300</sub> / PhoA <sub>22-472</sub> / LacZ <sub>4-60</sub> fusion protein <b>without the PelB</b> signal peptide                      | Membrane insertion   | This work study |
| pKTop:: <i>tse5-CT</i> <sub>1169-1317</sub>   | Derived from pKTop expressing the Tse5-CT <sub>1169-1317</sub> / PhoA <sub>22-472</sub> / LacZ <sub>4-60</sub> fusion protein <b>without the PelB</b> signal peptide                      | Membrane insertion   | This work study |
| pS238D1                                       | Vector optimized to express toxins in <i>P. putida</i> with transcriptional repression, pBBR1 oriV and oriT; Km <sup>r</sup>  | Parental vector  | 7               |
| pS238D1:: <i>tse5-CT</i>                      | Derived from pS238D1 that expresses the protein Tse5-CT <sub>1169-1317</sub>  | Biological function  | This work study |

|   |   |   |              |
|---|---|---|--------------|
| <b>pS238D1::sptse5-CT</b>   | Derived from pS238D1 that expresses the Tse5-CT <sub>1169-1317</sub> protein with the PelB signal peptide fused at the N-terminus                       | Biological function study   | This work    |
| <b>pSEVA424</b>   | Vector for protein expression in a broad-spectrum of organisms, oriV and oriT; Str <sup>r</sup>   | Parental vector   | <sup>8</sup> |
| <b>pSEVA424::tsi5</b>   | Derived from pSEVA <sub>424</sub> that expresses the protein Tsi5 <sub>1-76</sub>   | Biological function study   | This work    |
| <b>pS238D1::sptse5-CT<sub>1169-1317</sub>-phoA-lacZ<sub>a</sub></b> | The gene coding for spTse5-CT <sub>1169-1317</sub> -PhoA <sub>22-474</sub> -LacZ <sub>4-60</sub> fusion protein was subcloned into the pS238D1 plasmid. | Test the biological function of the spTse5-CT <sub>1169-1317</sub> -PhoA <sub>22-474</sub> -LacZ <sub>4-60</sub> fusion protein in <i>P. putida</i> | This work    |
| <b>pET29a(+):9xhis-Tse5</b>   | Plasmid harbouring a construct based on tse5 and coding for a 9xHis tag and a tobacco etch virus protease cleavage site at the 5' end.                  | Heterologous expression of Tse5 in <i>E. coli</i> Lemo21 cells for purification of Tse5-CT  | This work    |
| <b>pET29a(+):D1141A</b>   | Plasmid derived from pET29a(+):9xhis-Tse5 coding for a D1141A point mutation.   | Test the activity of the putative aspartyl protease motif DPXGL-(18)-DPXGL  | This work    |
| <b>pET29a(+):D1164A</b>   | Plasmid derived from pET29a(+):9xhis-Tse5 coding for a D1164A point mutation.   | Test the activity of the putative aspartyl protease motif DPXGL-(18)-DPXGL  | This work    |

## Supplementary Figures

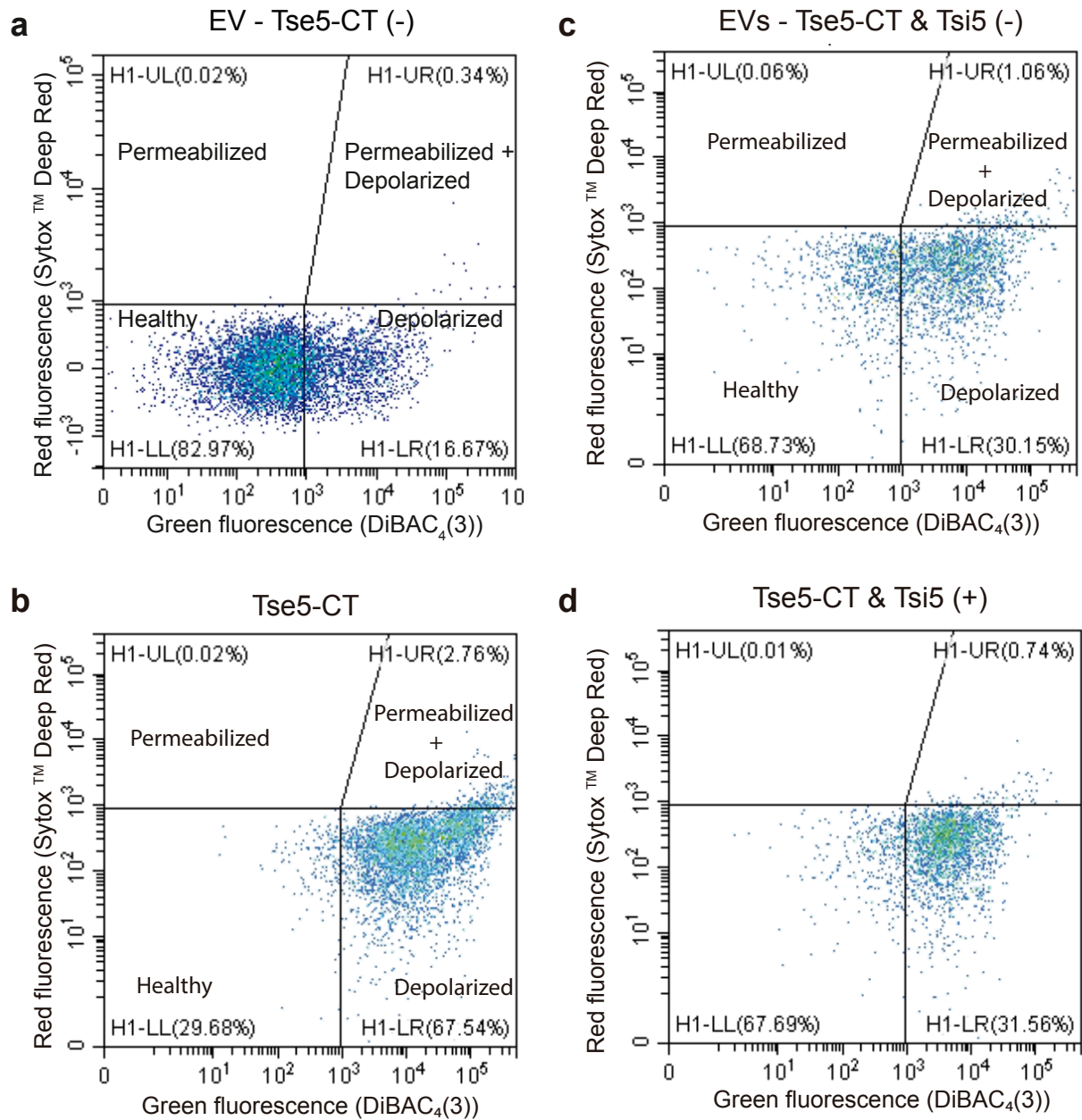


**Supplementary Fig. 1 | Competition assays between *P. aeruginosa* PAO1 *retS* attacker strains and *P. putida* KT2440R prey strain.** The prey strain harbors a mini-Tn7 transposon inserted on the chromosome that confers gentamycin resistance. The *P. aeruginosa* PAO1 *retS* (parental strain) and its isogenic *vgrG1* and *tse5* mutants were co-incubated with *P. putida* KT2440R for 5 hours. Colony-forming unit (CFU) quantifications of the prey survival after competition were performed on gentamycin selection. Graph shows means  $\pm$ SD, significance is indicated by \*\* if  $p < 0.01$ , \*\*\* if  $p < 0.001$  or \*\*\*\* if  $p < 0.0001$ . Statistical analysis was performed using RM one-way ANOVA multiple comparison (n=17).

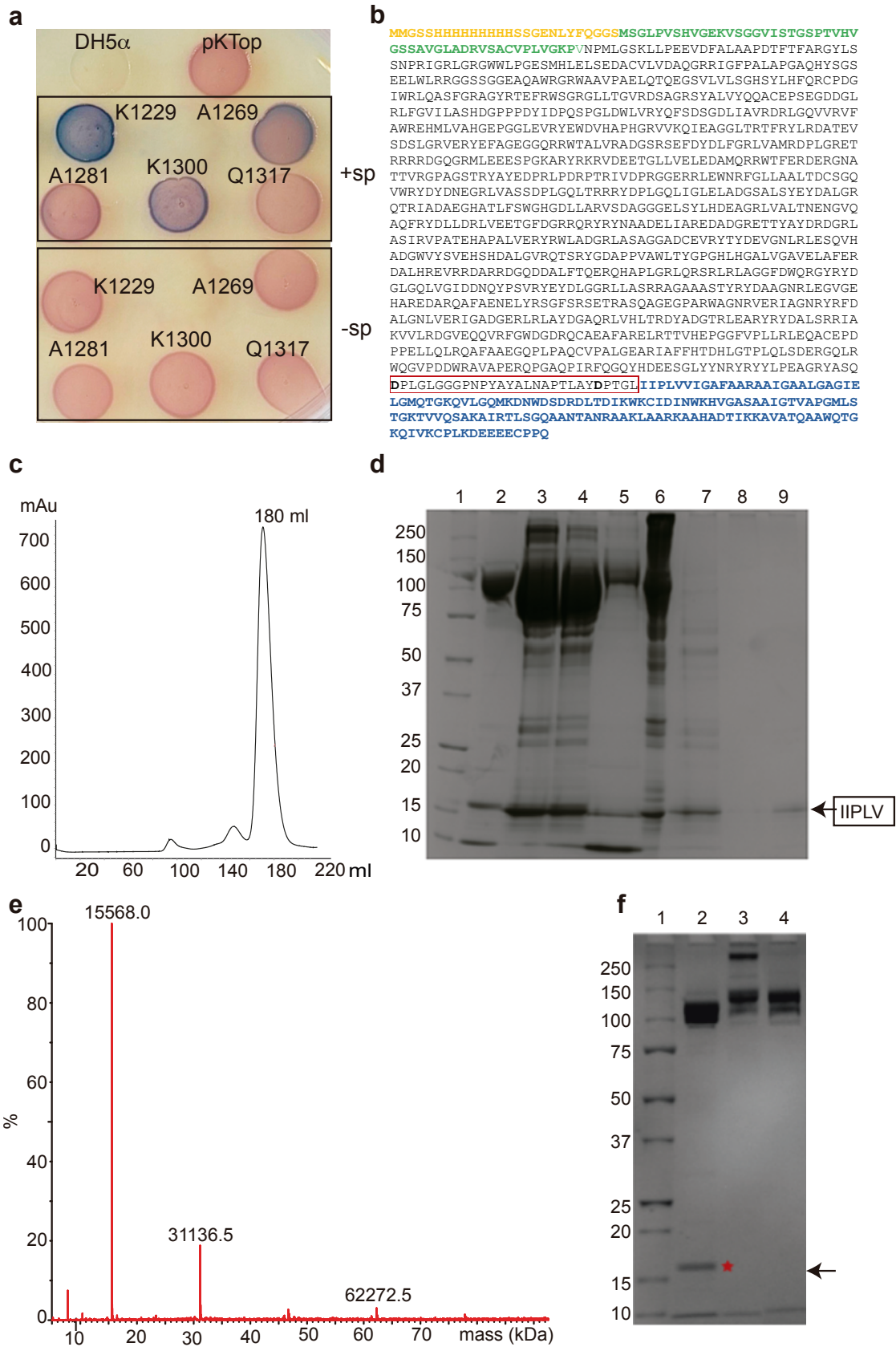


**Supplementary Fig. 2 | Analysis of bacterial control cells by Flow Cytometry** **a.** *P. putida* cells gating to classify cell size and complexity, with the X-axis being the size (FSC channel) and the Y-axis is the complexity (SSC channel). **b.** Not treated cells to identify healthy population. **c.** Cells treated with polymyxin B (100 µg/ml) to classify the depolarized population. **d.** Cells treated with heat shock to classify the permeabilized population. **e.** Cells treated with polymyxin B (100 µg/ml) and heat shock to identify depolarized and permeabilized population. Red fluorescence emitted by the Sytox™ Deep Red fluorescent marker (APC channel), a cell permeability marker, is represented on the X-axis, while the green fluorescence obtained by the DiBAC<sub>4</sub>(3) marker (FITC channel), a fluorophore sensitive to membrane depolarization.



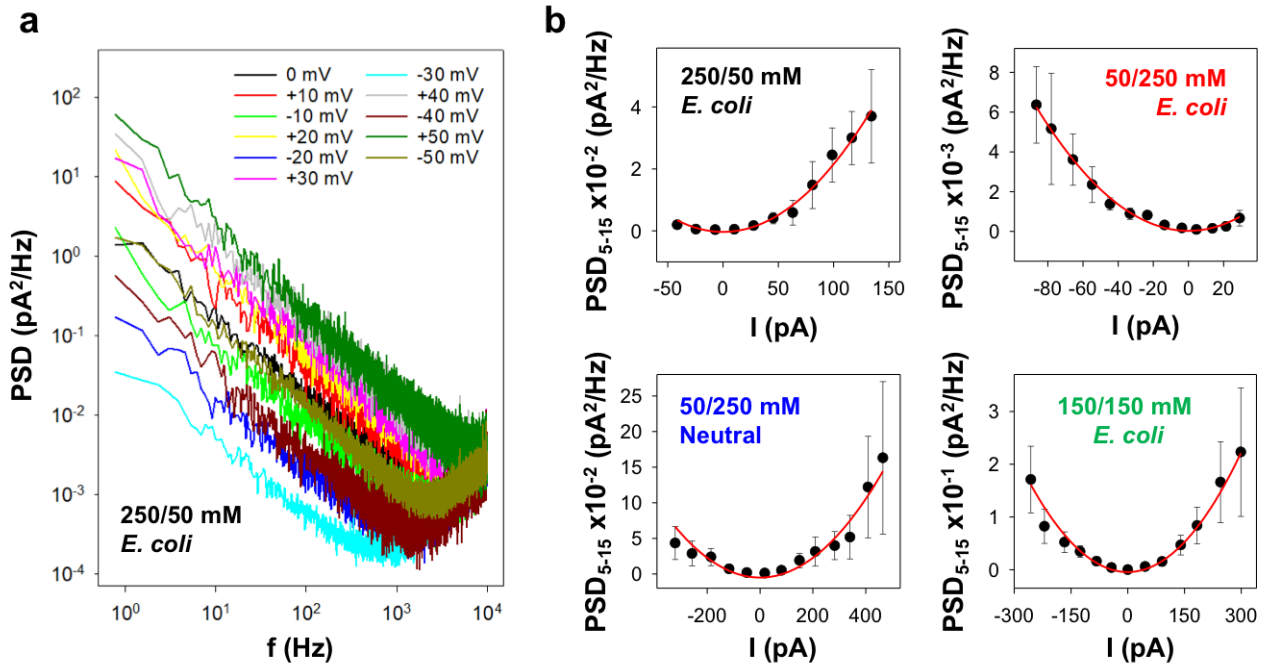


**Supplementary Fig. 3 | Bacterial cell analysis by Flow Cytometry reveal Tse5-CT causes membrane depolarization, and Tsi5 can protect from Tse5-induced effect.** **a.** Empty vector carrying cells to identify basally permeabilized or/and depolarized cell populations. **b.** *P. putida* cells expressing Tse5-CT. **c.** *P. putida* cells expressing spTse5-CT, which translocate to the periplasm through the SEC pathway. **d.** *P. putida* cells expressing Tse5-CT and Tsi5.

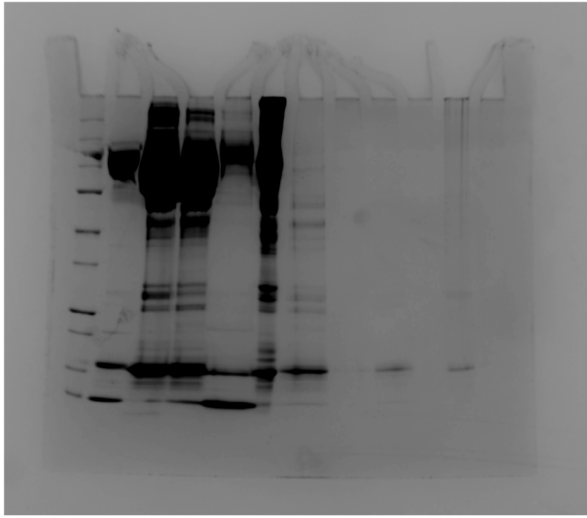
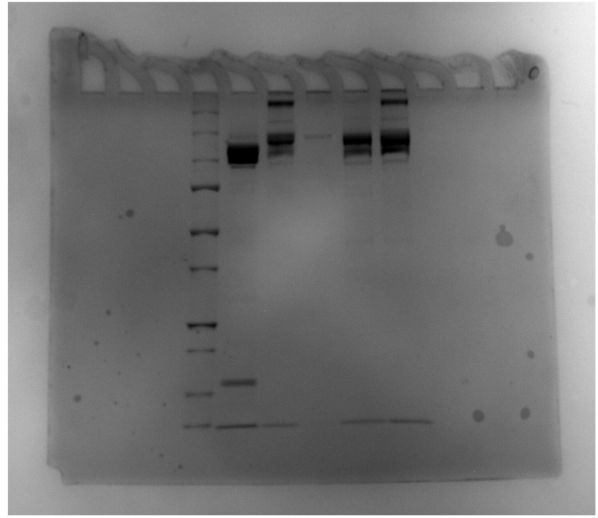


**Supplementary Fig. 4 | PhoA-LacZ dual reporter strategy for topology analysis, Tse5/Tse5-CT protein purification analysis, and autoproteolytic activity of Tse5. a.** In the absence of a signal

peptide (-sp), the reporter PhoA-LacZ $\alpha$  fusion always remains in the cytosol. *E. coli* DH5 $\alpha$  cells transformed with spTse5-CT-PhoA-LacZ $\alpha$  and Tse5-CT-PhoA-LacZ $\alpha$  fusion proteins growing on dual reporter agar plates. In the absence of a signal peptide (-sp), the reporter PhoA-LacZ $\alpha$  fusion remains in the cytosol independently of the Tse5-CT fusion point. As a result, the colonies growing on dual reporter LB agar plates are always coloured in red as a result of the  $\beta$ -galactosidase activity of LacZ. **b.** The protein sequence of Tse5 full length construct used in this study for heterologous expression in *E. coli* Lemo21 cells. The construct contains a 9xhis-tag at the N-terminus to facilitate the purification, coloured in yellow. The three predicted domains of Tse5 are indicated in different colours: The N-terminal domain in green, the Rhs domain in black and the Tse5-CT sequence in blue. The conserved motif that forms the active site of a putative aspartyl protease that releases the C-terminal is delimited by a red rectangle, with the two aspartic residues highlighted in bold (D1141 and D1164). **c.** Purified Tse5 behaves in solution as a monodisperse protein. Size exclusion chromatography (Superdex 200 26/600) of the Tse5 full-length protein expressed in *E. coli* Lemo21 cells shows an elution peak at 180 mL, which according to molecular weight standards approximates to a Tse5 monomer (146 kDa). **d.** Tse5-CT can be purified from Tse5 following protein denaturation and precipitation. Sodium dodecyl sulfate-polyacrylamide gel electrophoresis (SDS-PAGE) analysis of Tse5-CT purification (4-20% gel (ExpressPlus™ PAGE Gel, GenScript). Lane 1, molecular weight standard (Precision Plus Protein™ Standards, BIO-RAD); Lane 2, pure Tse5 full length; Lane 3, Tse5 dissolved in buffer A with 8M urea; Lane 3, unbound fraction of the nickel resin; Lane 4, 100% B elution of the nickel resin; Lane 5, the pellet of 0.9M ammonium sulphate precipitation; Lane 7, supernatant of 0.9 M ammonium sulphate precipitation; Lane 8, supernatant of wash steps; Lane 9, pure Tse5-CT. The N-terminal sequence of Tse5-CT was confirmed to be **IPLV** by N-terminal Edman sequencing (sequence indicated in the SDS-PAGE gel). **e.** Mass Spectrometry analysis confirms the identity of purified Tse5-CT. The identity of the purified Tse5-CT protein (see lane 9 in the SDS-PAGE (panel (d)) was confirmed by MS analysis. The major peak corresponds to Tse5-CT (the calculated mass for Tse5-CT is 15571.02 Da), while the other two peaks approximate to the molecular weight of the dimer and trimer, respectively. **f.** Single point mutants of putative catalytic residues D1141A and D1164A are unable to cleave Tse5 to release the Tse5-CT. SDS-PAGE analysis of Tse5, D1141A, and D1164A purifications (4-20% gel (ExpressPlus™ PAGE Gel, GenScript). Line 1, molecular weight standard (Precision Plus Protein™ Standards, BIO-RAD); Lane 2, purified Tse5 full length showing the Tse5-CT above the 15 kDa marker (red star); Lane 3, purified D1141A mutant; Line 4, purified D1164A mutant. Both mutants are unable to cleave the Tse5-CT.





**Supplementary Fig. 5 | Tse5-CT-induced currents display 1/f power spectral densities and equilibrium conductance fluctuations. a.** Representative PSDs as a function of frequency obtained from Tse5-CT-induced currents in 250/50 mM KCl gradient and using a polar lipid extract from *E. coli* to form the membrane. **b.** Each curve corresponds to a different applied voltage, as indicated. Averaged PSD at the 5-15 Hz band as a function of the measured current obtained from PSDs (a) for the different explored conditions, as indicated. Solid lines represent a parabolic fitting.

**a****b**

**Supplementary Fig. 6 | Uncropped and unedited SDS-gels shown in Supplementary Fig. 3. a.** Sodium dodecyl sulfate-polyacrylamide gel electrophoresis (SDS-PAGE) analysis of Tse5-CT purification. **b.** SDS-PAGE analysis of Tse5, D1141A, and D1164A purifications.

# Supplementary Note 1 LC-ESI-MS report for Tse5-CT



functional genomics center zurich  
f . g . c . z

*Protein and Proteomics analyses  
Functional Genomics Center Zurich  
UZH/ETH Zürich  
Winterthurerstrasse 190  
CH-8057  
Dr. Serge Chesnov  
+41 44 635 39 50*

|                            |                                 |
|----------------------------|---------------------------------|
| <b>Requested analysis:</b> | <b>Protein Characterisation</b> |
| <b>Order/Sample:</b>       | 24894/ 4 samples                |
| <b>Customer:</b>           | David Albesa-Jove               |
| <b>Date:</b>               | 26/05/2021                      |
| <b>Analysis ID:</b>        | 20210525                        |

**Procedure**

Due to high sample heterogeneity (proven by direct-infusion ESI-MS), the samples were analysed in an LC-ESI-MS approach.

The samples were 3- resp. 2-fold diluted with 1% TFA and transferred to an autosampler vial for LC/MS. 7 ul resp. 10 ul of sample were injected into an ACQUITY UPLC@ BioResolve-RP-mAb 2.7µ 2.1x150 450 A (Waters, USA) column. For separation and elution on an Acquity UPLC station, a gradient buffer A (0.1% FA in water)/ buffer B (0.1% FA in AN) at a flow rate 200ul/min at 50°C over 25 min was applied.

| Time    | Flow (ml/min) | %A | %B | Curve   |
|---------|---------------|----|----|---------|
| Initial | 0.2           | 85 | 15 | Initial |
| 3.0     | 0.2           | 45 | 55 | 6       |

• • •  
1

|      |     |    |    |   |
|------|-----|----|----|---|
| 20.3 | 0.2 | 20 | 80 | 6 |
| 21.3 | 0.2 | 85 | 15 | 6 |
| 25   | 0.2 | 85 | 15 | 6 |

The analysis was performed on a Synapt G2 mass spectrometer directly coupled to the UPLC station.

Mass spectra were acquired in the positive-ion mode by scanning the  $m/z$  range from 100 to 4000 da with a scan duration of 1 s and an interscan delay of 0.1s. The spray voltage was set to 3 kV, the cone voltage to 50V, and the source temperature to 80 °C. The data were recorded with the MassLynx 4.2 Software (both Waters, UK). Where possible, the recorded  $m/z$  data of single peaks were deconvoluted into mass spectra by applying the maximum entropy algorithm MaxEnt1 (MaxLynx) with a resolution of the output mass 0.5 Da/channel and Uniform Gaussian Damage Model at the half height of 0.5 Da.

### Useful links

- [Free Scaffold viewer](#)
- [FGCZ intranet pages: Frequently Asked Questions](#)
  - [FGCZ Quick Scaffold guide \(how to access the most relevant Scaffold features\)](#)
- Tools for analyses of pull-down experiments
  - [String](#): Protein-Protein interaction networks
- [ExPASy tools](#) for proteomics
  - [PeptideCutter](#)
  - [PeptideMass](#)
- [Uniprot](#)
- Human repositories
  - [NextProt](#): Exploring the universe of human proteins

- [ProteomicsDB](#): expedite the identification of the human proteome
- [PaxDb](#): Protein Abundance Database

### Frequently asked questions (FAQs):

Please refer to our [FAQ pages](#) within the FGCZ intranet page.

If you do not find an answer to your questions, please contact us using the Comment functionality within your B-Fabric order.

For questions not related to a specific order, please send an email to:

[proteomics@fgcz.ethz.ch](mailto:proteomics@fgcz.ethz.ch)

### FGCZ policies

Unless stated otherwise, all the analyses have been performed under the [FGCZ Terms and Conditions](#).

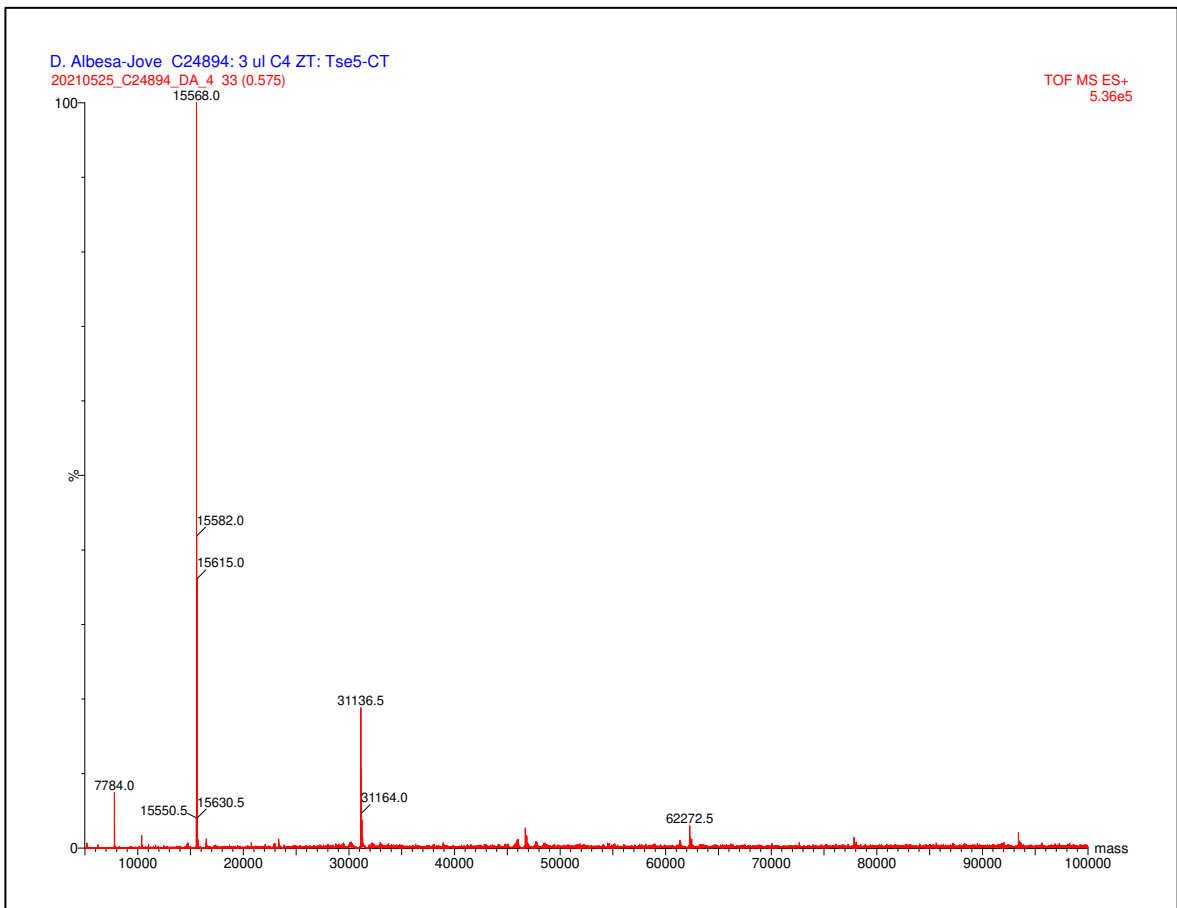
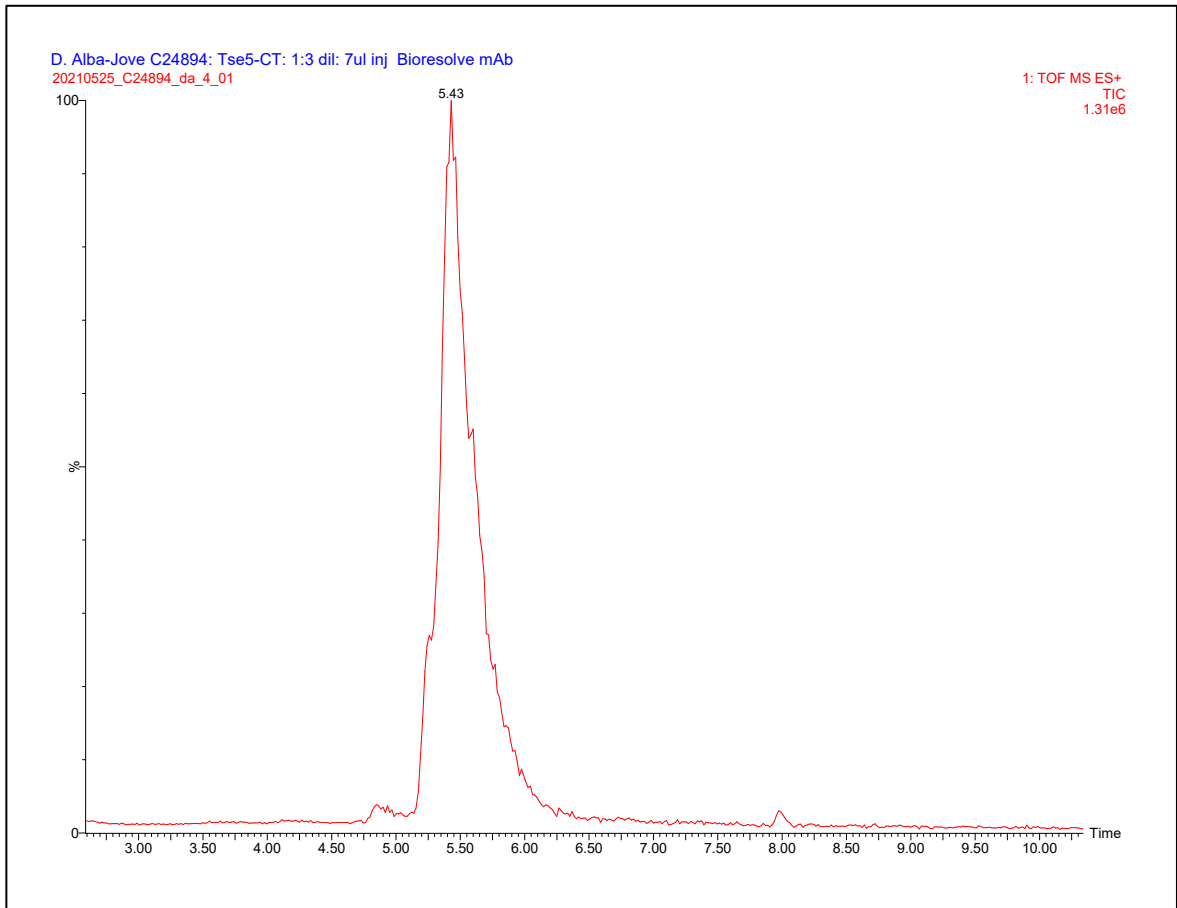
In case of full or partial publication of the results, please acknowledge the FGCZ for the analyses and the technical support (Functional Genomics Center Zurich (FGCZ), University/ETH Zurich).

All the unused samples are discarded 4 week after analyses.

### Data

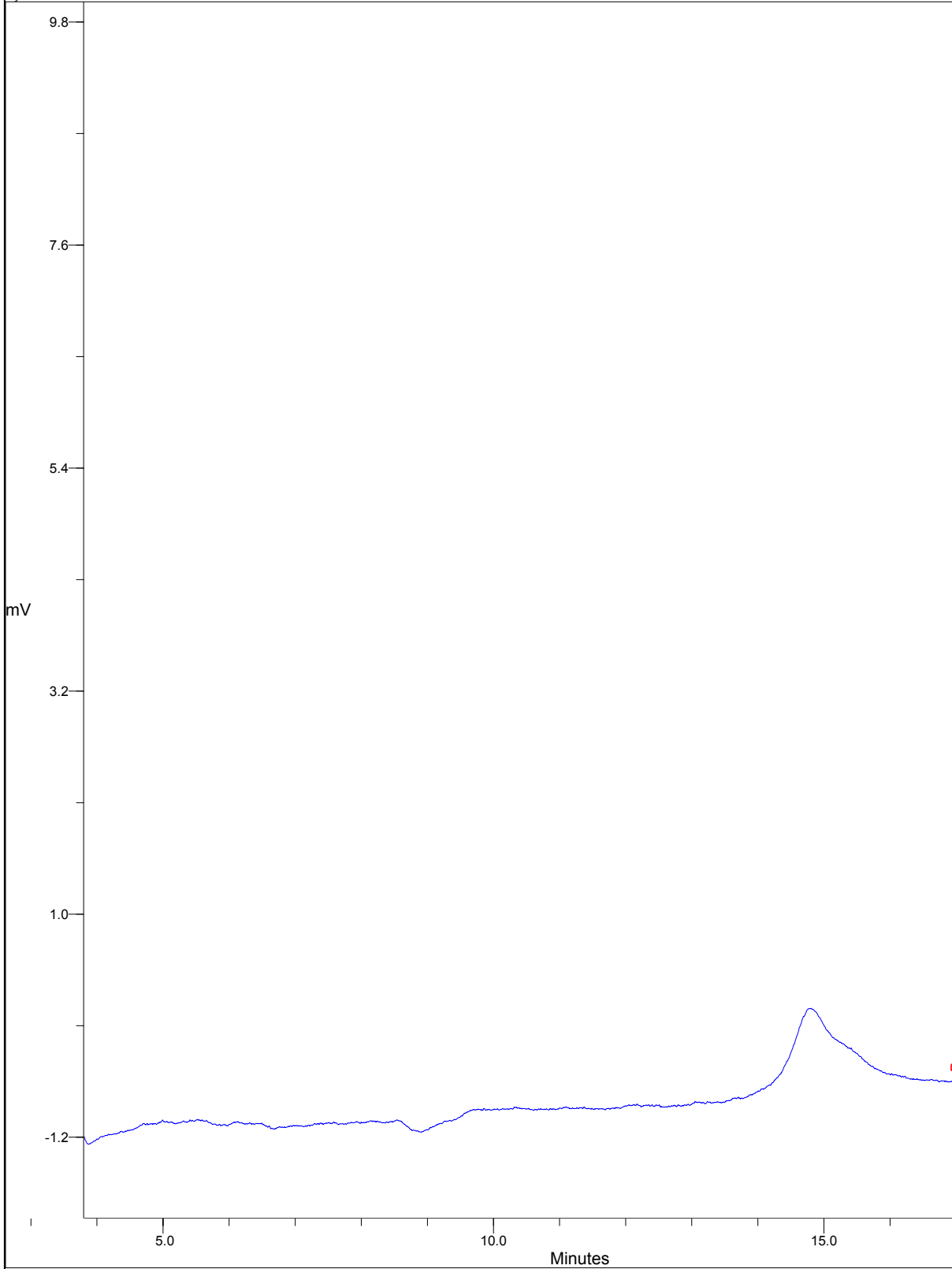
The following pages show the results of the requested analyses.



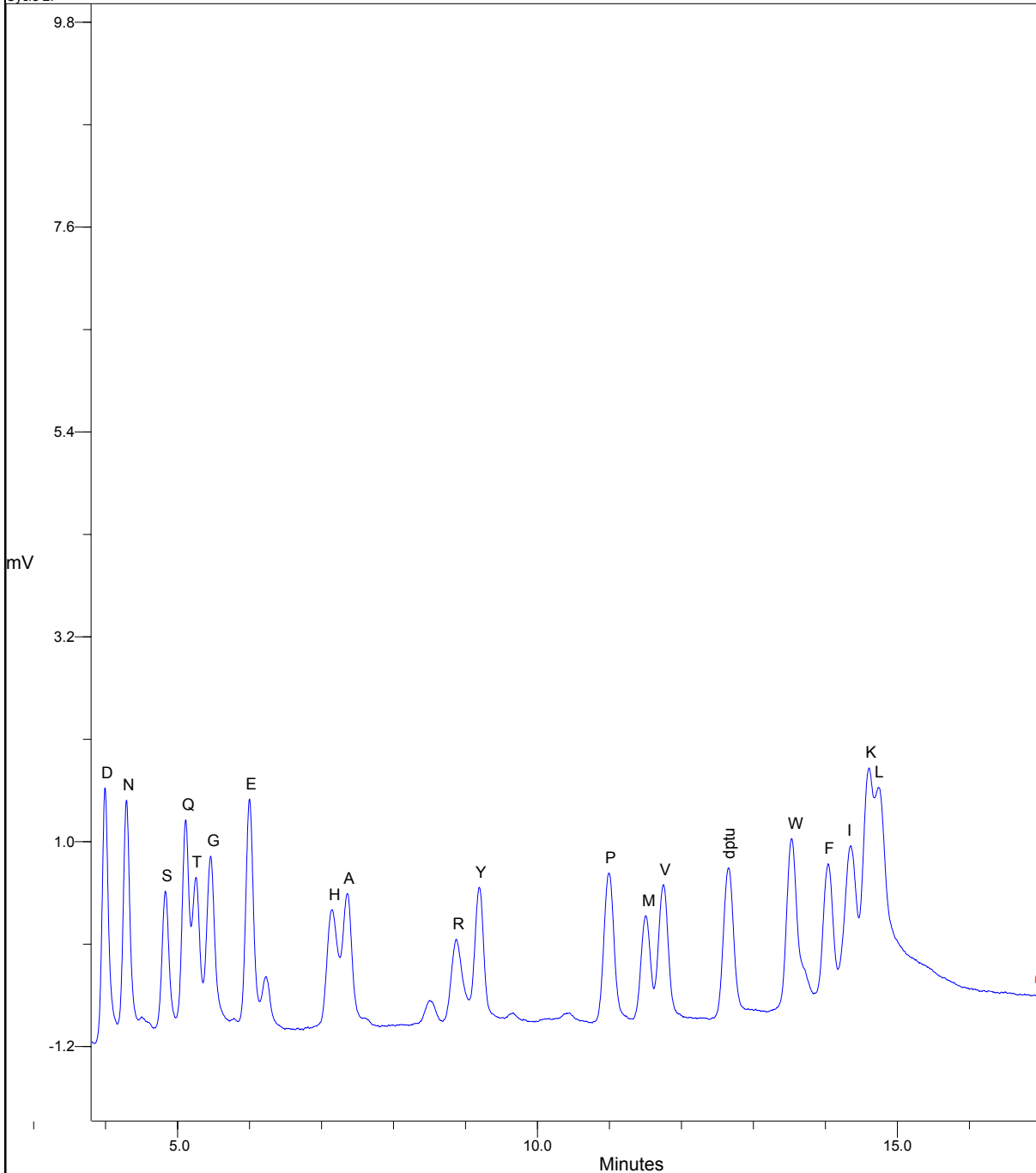




Cycle 1:Blank 1



Cycle 2:

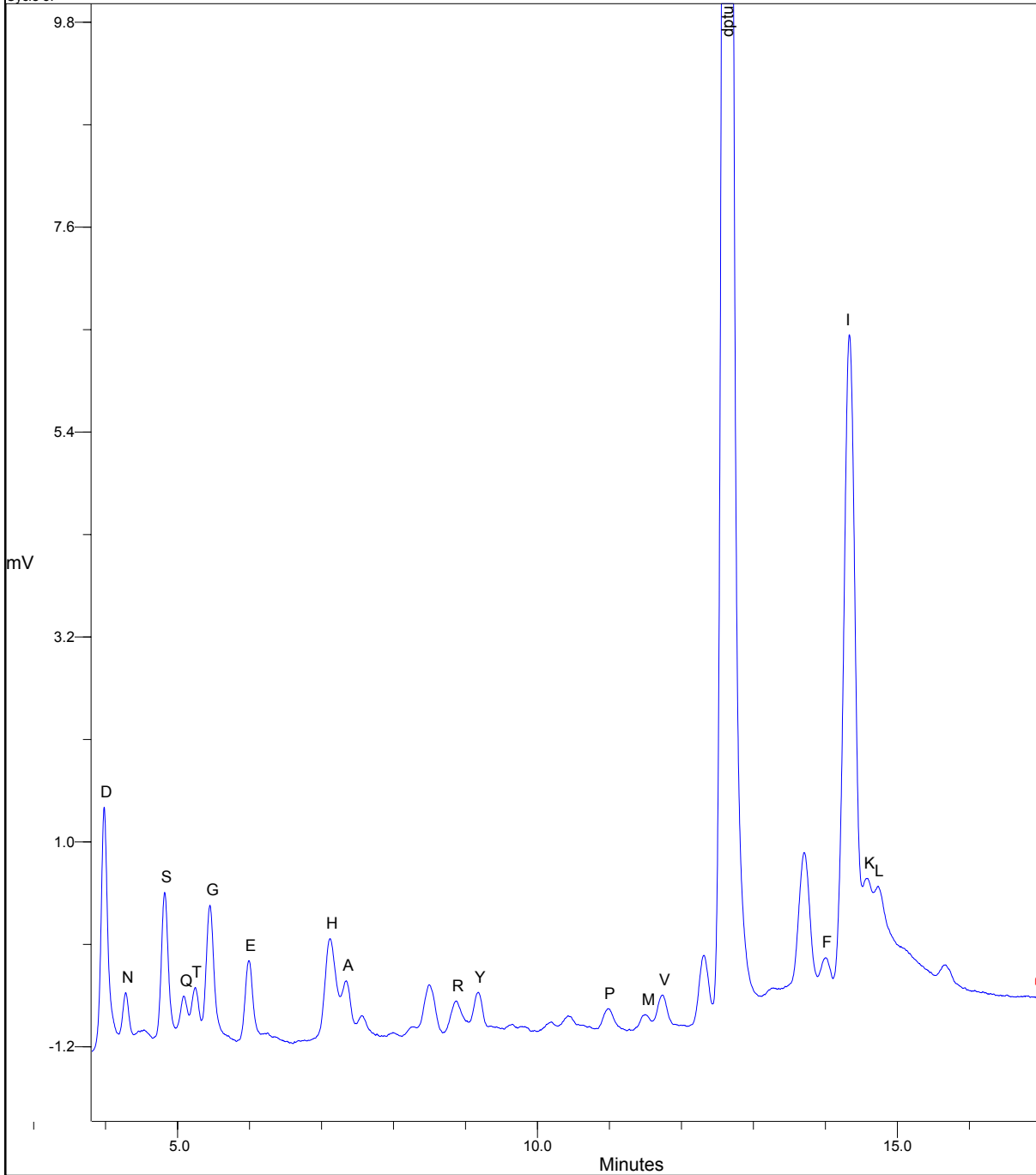


| PEAK ID | R.TIME (mins) | C.TIME (mins) | HEIGHT (mV) | PMOL HT | PEAK ID | R.TIME (mins) | C.TIME (mins) | HEIGHT (mV) | PMOL HT |
|---------|---------------|---------------|-------------|---------|---------|---------------|---------------|-------------|---------|
| D       | 3.99          | 3.99          | 2.741       | 8.000   | Y       | 9.19          | 9.19          | 1.453       | 8.000   |
| N       | 4.29          | 4.29          | 2.591       | 8.000   | P       | 10.99         | 10.99         | 1.605       | 8.000   |
| S       | 4.83          | 4.83          | 1.582       | 8.000   | M       | 11.50         | 11.50         | 1.129       | 8.000   |
| Q       | 5.11          | 5.11          | 2.333       | 8.000   | V       | 11.75         | 11.75         | 1.453       | 8.000   |
| T       | 5.25          | 5.25          | 1.704       | 8.000   | dptu    | 12.66         | 12.66         | 1.575       | 8.000   |
| G       | 5.46          | 5.46          | 1.922       | 8.000   | W       | 13.53         | 13.53         | 1.814       | 8.000   |
| E       | 6.00          | 6.00          | 2.505       | 8.000   | F       | 14.04         | 14.04         | 1.469       | 8.000   |
| H       | 7.15          | 7.15          | 1.232       | 8.000   | I       | 14.35         | 14.35         | 1.615       | 8.000   |
| A       | 7.36          | 7.36          | 1.374       | 8.000   | K       | 14.61         | 14.61         | 2.415       | 8.000   |
| R       | 8.87          | 8.87          | 0.908       | 8.000   | L       | 14.74         | 14.74         | 2.186       | 8.000   |

Wednesday, March 09, 2022 09:49:16

David Albesa\_Cterminal - 08Mar2022 10-09-34 - Page 3 of 8

Cycle 3:

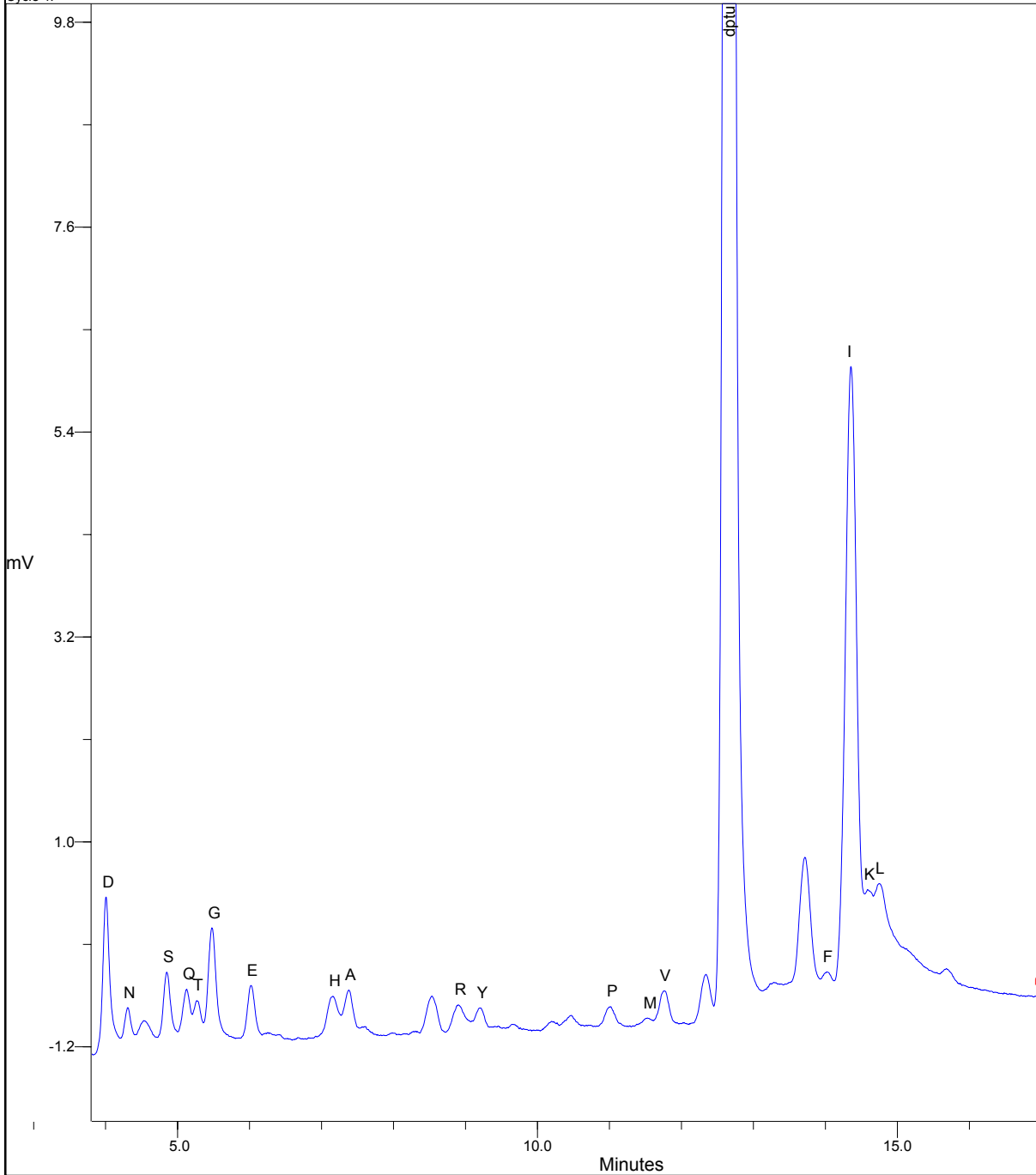


| PEAK ID | R.TIME (mins) | C.TIME (mins) | HEIGHT (mV) | PMOL HT | PEAK ID | R.TIME (mins) | C.TIME (mins) | HEIGHT (mV) | PMOL HT |
|---------|---------------|---------------|-------------|---------|---------|---------------|---------------|-------------|---------|
| D       | 3.98          | 3.99          | 2.616       | 7.636   | Y       | 9.18          | 9.19          | 0.399       | 2.196   |
| N       | 4.28          | 4.29          | 0.612       | 1.888   | P       | 10.98         | 10.99         | 0.241       | 1.203   |
| S       | 4.82          | 4.83          | 1.657       | 8.382   | M       | 11.50         | 11.50         | 0.157       | 1.115   |
| Q       | 5.08          | 5.11          | 0.529       | 1.815   | V       | 11.74         | 11.75         | 0.348       | 1.915   |
| T       | 5.25          | 5.25          | 0.613       | 2.878   | dptu    | 12.64         | 12.66         | 27.562      | 139.970 |
| G       | 5.45          | 5.46          | 1.486       | 6.186   | F       | 14.00         | 14.04         | 0.580       | 3.157   |
| E       | 5.99          | 6.00          | 0.858       | 2.740   | I       | 14.33         | 14.35         | 7.242       | 35.866  |
| H       | 7.12          | 7.15          | 1.089       | 7.067   | K       | 14.59         | 14.61         | 0.921       | 3.051   |
| A       | 7.35          | 7.36          | 0.618       | 3.600   | L       | 14.73         | 14.74         | 1.192       | 4.361   |
| R       | 8.87          | 8.87          | 0.329       | 2.903   |         |               |               |             |         |

Wednesday, March 09, 2022 09:49:17

David Albesa\_Cterminal - 08Mar2022 10-09-34 - Page 4 of 8

Cycle 4:

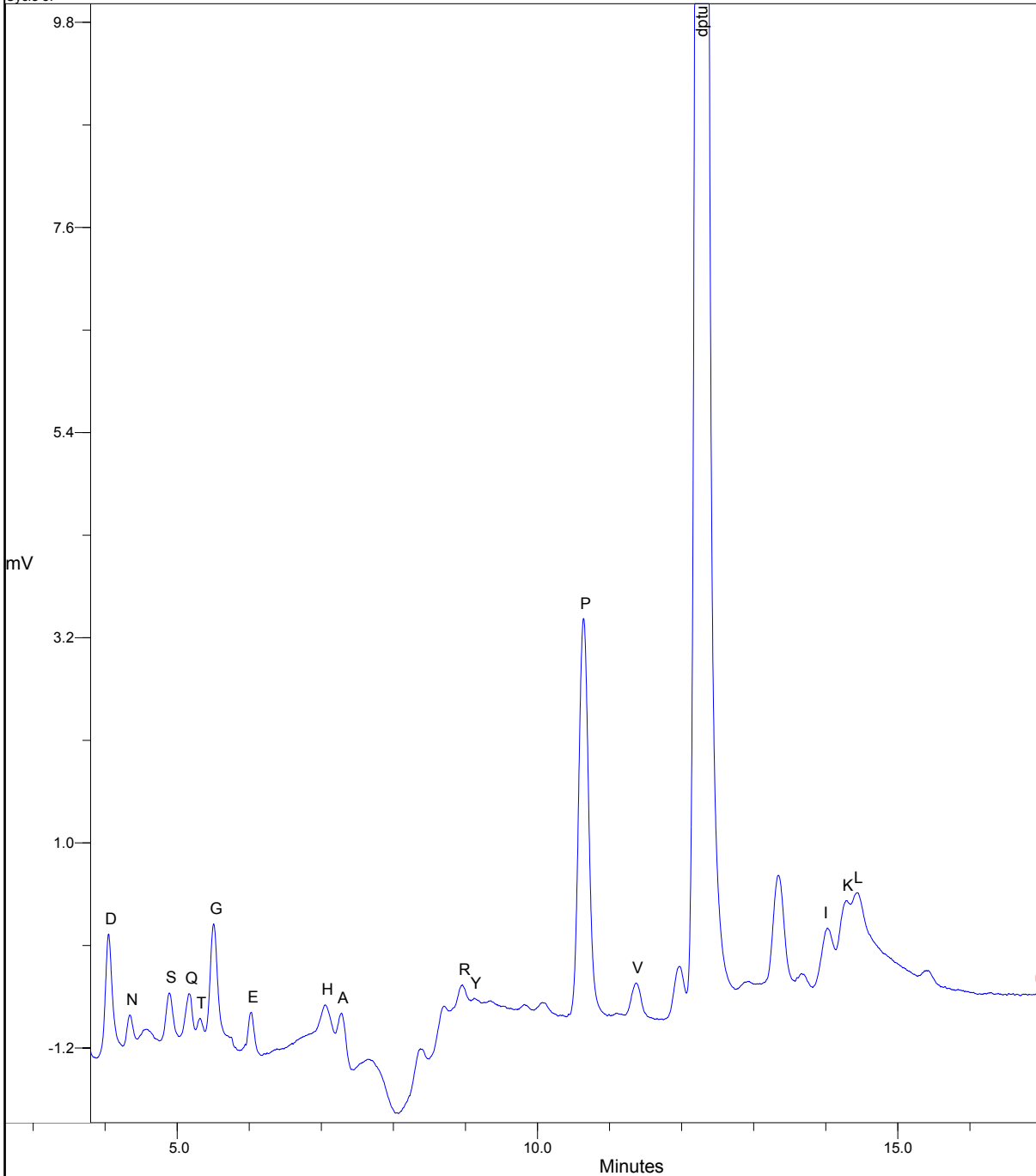


| PEAK ID | R.TIME (mins) | C.TIME (mins) | HEIGHT (mV) | PMOL HT | PEAK ID | R.TIME (mins) | C.TIME (mins) | HEIGHT (mV) | PMOL HT |
|---------|---------------|---------------|-------------|---------|---------|---------------|---------------|-------------|---------|
| D       | 4.01          | 3.99          | 1.688       | 4.928   | Y       | 9.21          | 9.19          | 0.221       | 1.218   |
| N       | 4.30          | 4.29          | 0.480       | 1.481   | P       | 11.02         | 10.99         | 0.216       | 1.078   |
| S       | 4.85          | 4.83          | 0.824       | 4.170   | M       | 11.53         | 11.50         | 0.090       | 0.638   |
| Q       | 5.13          | 5.11          | 0.624       | 2.141   | V       | 11.75         | 11.75         | 0.373       | 2.052   |
| T       | 5.27          | 5.25          | 0.492       | 2.309   | dptu    | 12.66         | 12.66         | 35.895      | 182.288 |
| G       | 5.47          | 5.46          | 1.261       | 5.249   | F       | 14.02         | 14.04         | 0.383       | 2.085   |
| E       | 6.02          | 6.00          | 0.606       | 1.934   | I       | 14.35         | 14.35         | 6.850       | 33.921  |
| H       | 7.15          | 7.15          | 0.449       | 2.914   | K       | 14.59         | 14.61         | 0.664       | 2.201   |
| A       | 7.38          | 7.36          | 0.506       | 2.948   | L       | 14.75         | 14.74         | 1.165       | 4.263   |
| R       | 8.90          | 8.87          | 0.281       | 2.477   |         |               |               |             |         |

Wednesday, March 09, 2022 09:49:17

David Albesa\_Cterminal - 08Mar2022 10-09-34 - Page 5 of 8

Cycle 5:

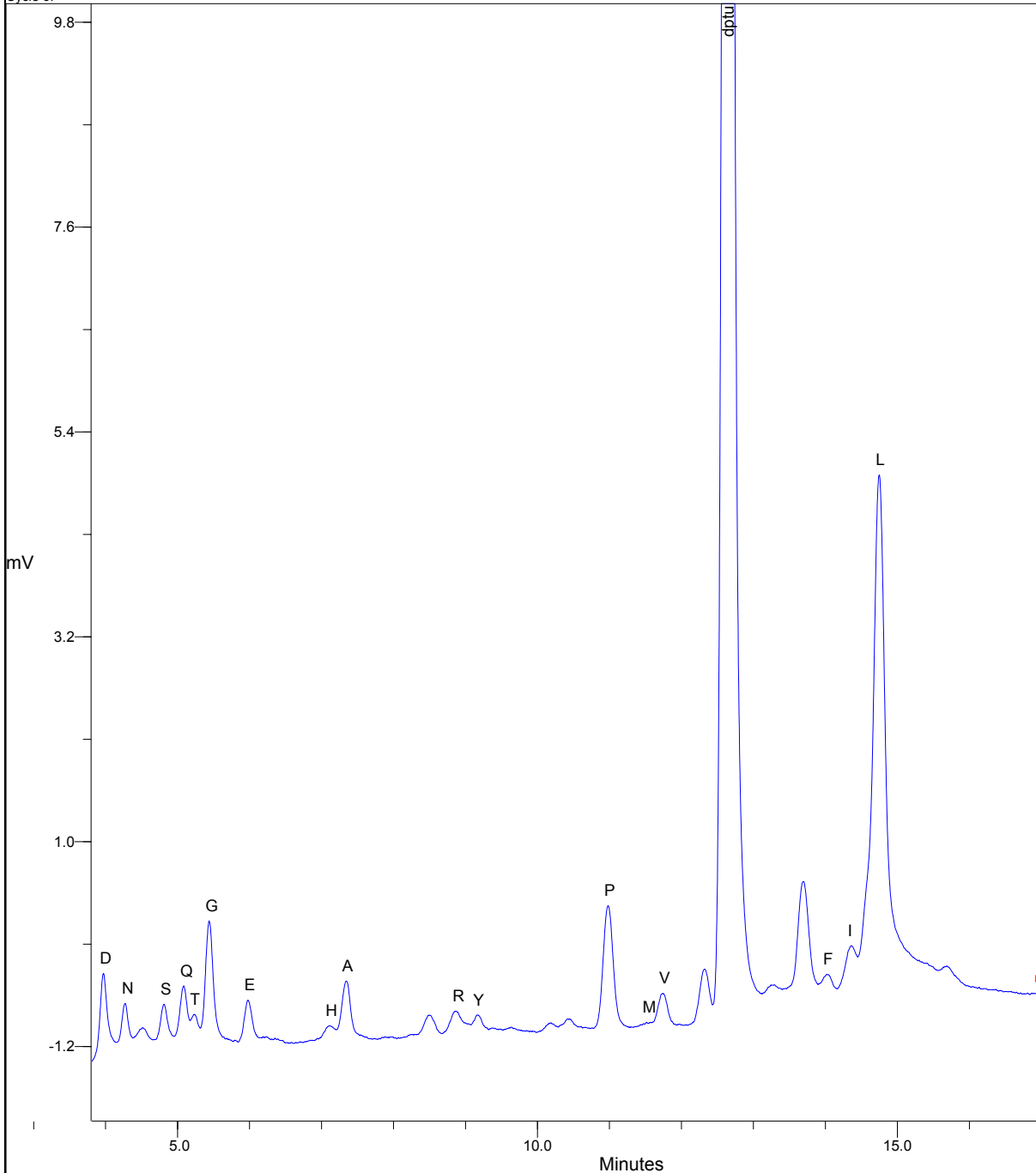


| PEAK ID | R.TIME (mins) | C.TIME (mins) | HEIGHT (mV) | PMOL HT | PEAK ID | R.TIME (mins) | C.TIME (mins) | HEIGHT (mV) | PMOL HT |
|---------|---------------|---------------|-------------|---------|---------|---------------|---------------|-------------|---------|
| D       | 4.05          | 3.99          | 1.361       | 3.973   | Y       | 9.12          | 9.19          | 0.304       | 1.671   |
| N       | 4.35          | 4.29          | 0.532       | 1.643   | P       | 10.64         | 10.99         | 4.281       | 21.339  |
| S       | 4.89          | 4.83          | 0.846       | 4.279   | V       | 11.37         | 11.75         | 0.386       | 2.125   |
| Q       | 5.16          | 5.11          | 0.876       | 3.006   | dptu    | 12.28         | 12.66         | 38.326      | 194.635 |
| T       | 5.32          | 5.25          | 0.635       | 2.979   | I       | 14.02         | 14.35         | 0.784       | 3.882   |
| G       | 5.50          | 5.46          | 1.675       | 6.974   | K       | 14.28         | 14.61         | 1.055       | 3.494   |
| E       | 6.03          | 6.00          | 0.799       | 2.553   | L       | 14.44         | 14.74         | 1.125       | 4.117   |
| H       | 7.05          | 7.15          | 1.024       | 6.650   |         |               |               |             |         |
| A       | 7.28          | 7.36          | 0.969       | 5.642   |         |               |               |             |         |
| R       | 8.96          | 8.87          | 0.537       | 4.727   |         |               |               |             |         |

Wednesday, March 09, 2022 09:49:18

David Albesa\_Cterminal - 08Mar2022 10-09-34 - Page 6 of 8

Cycle 6:



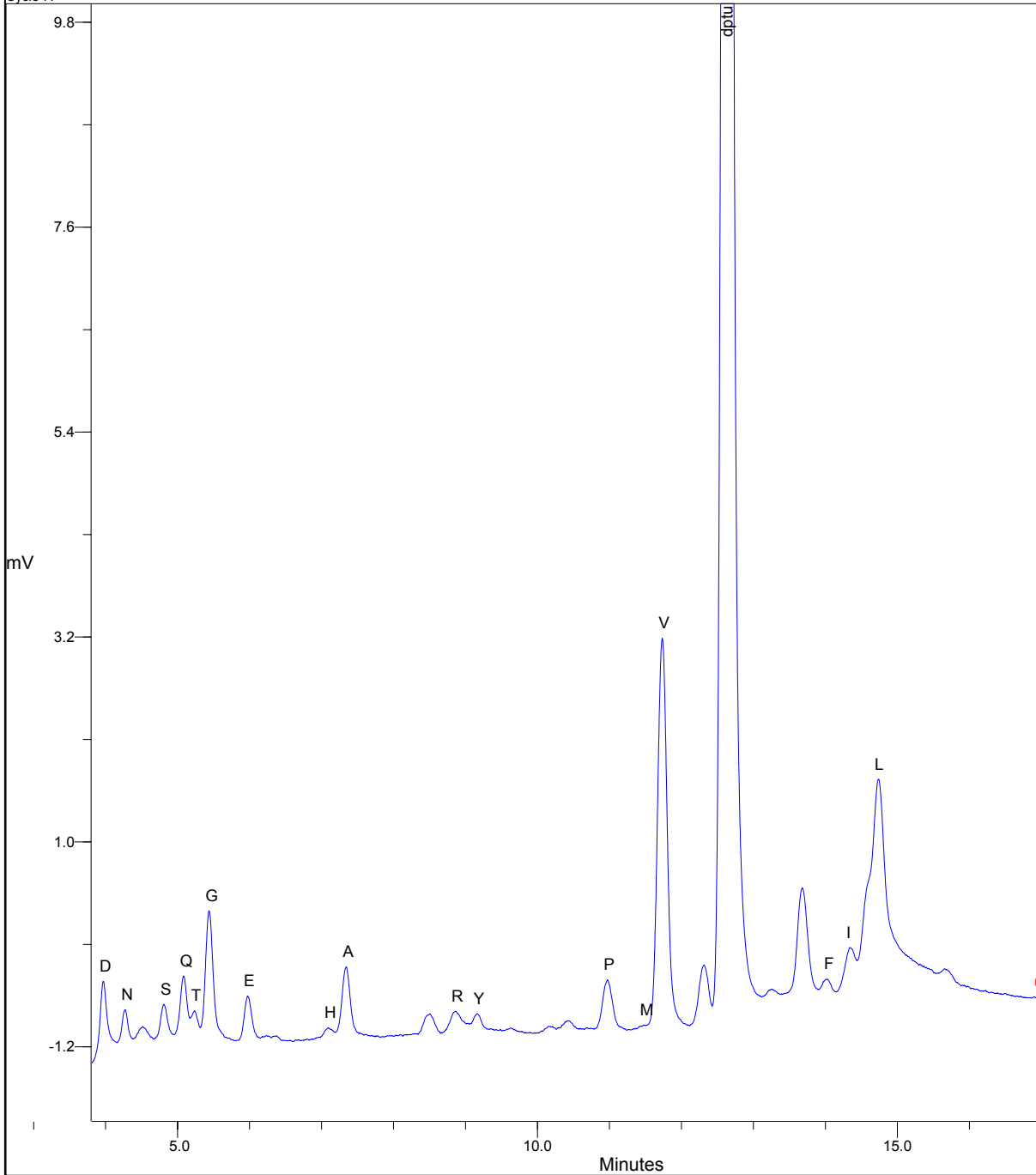
| PEAK ID | R.TIME (mins) | C.TIME (mins) | HEIGHT (mV) | PMOL HT | PEAK ID | R.TIME (mins) | C.TIME (mins) | HEIGHT (mV) | PMOL HT |
|---------|---------------|---------------|-------------|---------|---------|---------------|---------------|-------------|---------|
| D       | 3.97          | 3.99          | 0.930       | 2.714   | Y       | 9.16          | 9.19          | 0.205       | 1.126   |
| N       | 4.28          | 4.29          | 0.569       | 1.757   | P       | 10.98         | 10.99         | 1.316       | 6.560   |
| S       | 4.81          | 4.83          | 0.491       | 2.485   | M       | 11.51         | 11.50         | 0.050       | 0.355   |
| Q       | 5.09          | 5.11          | 0.654       | 2.243   | V       | 11.74         | 11.75         | 0.354       | 1.950   |
| T       | 5.22          | 5.25          | 0.330       | 1.550   | dptu    | 12.65         | 12.66         | 34.146      | 173.410 |
| G       | 5.44          | 5.46          | 1.309       | 5.449   | F       | 14.02         | 14.04         | 0.349       | 1.898   |
| E       | 5.98          | 6.00          | 0.429       | 1.370   | I       | 14.36         | 14.35         | 0.622       | 3.079   |
| H       | 7.11          | 7.15          | 0.175       | 1.133   | L       | 14.75         | 14.74         | 5.640       | 20.635  |
| A       | 7.34          | 7.36          | 0.646       | 3.760   |         |               |               |             |         |
| R       | 8.87          | 8.87          | 0.261       | 2.299   |         |               |               |             |         |

Wednesday, March 09, 2022 09:49:18

David Albesa\_Cterminal - 08Mar2022 10-09-34 - Page 7 of 8



Cycle 7:



| PEAK ID | R.TIME (mins) | C.TIME (mins) | HEIGHT (mV) | PMOL HT | PEAK ID | R.TIME (mins) | C.TIME (mins) | HEIGHT (mV) | PMOL HT |
|---------|---------------|---------------|-------------|---------|---------|---------------|---------------|-------------|---------|
| D       | 3.97          | 3.99          | 0.831       | 2.427   | Y       | 9.16          | 9.19          | 0.191       | 1.050   |
| N       | 4.27          | 4.29          | 0.435       | 1.342   | P       | 10.97         | 10.99         | 0.540       | 2.690   |
| S       | 4.81          | 4.83          | 0.378       | 1.910   | M       | 11.48         | 11.50         | 0.045       | 0.318   |
| Q       | 5.08          | 5.11          | 0.686       | 2.352   | V       | 11.73         | 11.75         | 4.183       | 23.036  |
| T       | 5.24          | 5.25          | 0.313       | 1.471   | dptu    | 12.63         | 12.66         | 33.180      | 168.502 |
| G       | 5.44          | 5.46          | 1.392       | 5.797   | F       | 14.03         | 14.04         | 0.161       | 0.878   |
| E       | 5.97          | 6.00          | 0.485       | 1.549   | I       | 14.34         | 14.35         | 0.436       | 2.158   |
| H       | 7.09          | 7.15          | 0.116       | 0.756   | L       | 14.74         | 14.74         | 2.157       | 7.892   |
| A       | 7.35          | 7.36          | 0.754       | 4.390   |         |               |               |             |         |
| R       | 8.86          | 8.87          | 0.231       | 2.032   |         |               |               |             |         |

Wednesday, March 09, 2022 09:49:18

David Albesa\_Cterminal - 08Mar2022 10-09-34 - Page 8 of 8

## Supplementary references

1. Bernal, P. *et al.* A novel stabilization mechanism for the type VI secretion system sheath. *Proc. Natl. Acad. Sci. U. S. A.* **118**, e2008500118 (2021).
2. Lambertsen, L., Sternberg, C. & Molin, S. Mini-Tn7 transposons for site-specific tagging of bacteria with fluorescent proteins. *Environ. Microbiol.* **6**, 726–732 (2004).
3. Schlegel, S. *et al.* Optimizing membrane protein overexpression in the Escherichia coli strain Lemo21(DE3). *J. Mol. Biol.* **423**, 648–659 (2012).
4. Martínez-García, E., Nickel, P. I., Aparicio, T. & de Lorenzo, V. Pseudomonas 2.0: Genetic upgrading of *P. putida* KT2440 as an enhanced host for heterologous gene expression. *Microb. Cell Fact.* **13**, 159 (2014).
5. Whitney, J. C. *et al.* Genetically distinct pathways guide effector export through the type VI secretion system. *Mol. Microbiol.* **92**, 529–542 (2014).
6. Karimova, G., Robichon, C. & Ladant, D. Characterization of YmgF, a 72-residue inner membrane protein that associates with the Escherichia coli cell division machinery. *J. Bacteriol.* **91**, 333–346 (2009).
7. Calles, B., Goñi-Moreno, Á. & Lorenzo, V. Digitalizing heterologous gene expression in Gram-negative bacteria with a portable ON/OFF module. *Mol. Syst. Biol.* **15**, e8777 (2019).
8. Silva-Rocha, R. *et al.* The Standard European Vector Architecture (SEVA): A coherent platform for the analysis and deployment of complex prokaryotic phenotypes. *Nucleic Acids Res.* **41**, D666–D675 (2013).